



OPEN ACCESS

EDITED BY

He Liu,
Jilin University, China

REVIEWED BY

Chao Yang,
Zhejiang Ocean University, China
Zhipeng Gu,
Sichuan University, China
Ke Wang,
Xi'an Jiaotong University, China

*CORRESPONDENCE

Weidong Leng,
Lengweidong68@163.com
Jie Luo,
Luojie_th67@163.com

SPECIALTY SECTION

This article was submitted to
Biomaterials,
a section of the journal
Frontiers in Bioengineering and
Biotechnology

RECEIVED 25 April 2022

ACCEPTED 28 June 2022

PUBLISHED 03 August 2022

CITATION

Yu H, Xia L, Leng X, Chen Y, Zhang L,
Ni X, Luo J and Leng W (2022), Improved
repair of rabbit calvarial defects with
hydroxyapatite/chitosan/
polycaprolactone composite scaffold-
engrafted EPCs and BMSCs.
Front. Bioeng. Biotechnol. 10:928041.
doi: 10.3389/fbioe.2022.928041

COPYRIGHT

© 2022 Yu, Xia, Leng, Chen, Zhang, Ni,
Luo and Leng. This is an open-access
article distributed under the terms of the
[Creative Commons Attribution License
\(CC BY\)](https://creativecommons.org/licenses/by/4.0/). The use, distribution or
reproduction in other forums is
permitted, provided the original
author(s) and the copyright owner(s) are
credited and that the original
publication in this journal is cited, in
accordance with accepted academic
practice. No use, distribution or
reproduction is permitted which does
not comply with these terms.

Improved repair of rabbit calvarial defects with hydroxyapatite/chitosan/polycaprolactone composite scaffold-engrafted EPCs and BMSCs

Hedong Yu^{1,2}, Lingyun Xia^{1,2}, Xieyuan Leng³, Yongji Chen^{1,2},
Li Zhang^{1,2}, Xiaobing Ni^{1,2}, Jie Luo^{4*} and Weidong Leng^{1,2*}

¹Department of Stomatology, Taihe Hospital, Hubei University of Medicine, Shiyan, China, ²Institute of Dental Research, School of Dentistry, Hubei University of Medicine, Shiyan, China, ³The First Clinical College, Anhui Medical University, Hefei, China, ⁴Department of Neurosurgery, Taihe Hospital, Hubei University of Medicine, Shiyan, China

Endothelial progenitor cells (EPCs) expressing vascular endothelial growth factor (VEGF) and platelet-derived growth factor (PDGF) and bone marrow mesenchymal stem cells (BMSCs) expressing endogenous bone morphogenetic protein-2 (BMP-2) play the important role in new bone formation. This study investigated the effects of a porous hydroxyapatite (HA)/chitosan (CS)/polycaprolactone (PCL) composite scaffold-engrafted EPCs and BMSCs on the expression of BMP-2, VEGF, and PDGF in the calvarial defect rabbit model *in vivo*. It showed that a three-dimensional composite scaffold was successfully constructed by physical interaction with a pore size of 250 μm . The HA/CS/PCL scaffold degraded slowly within 10 weeks and showed non-cytotoxicity. By X-ray, micro-CT examination, and H&E staining, compared with the HA/CS/PCL group, HA/CS/PCL + EPCs, HA/CS/PCL + BMSCs, and HA/CS/PCL + EPCs + BMSCs groups performed a more obvious repair effect, and the dual factor group presented particularly significant improvement on the percentages of bone volume at week 4 and week 8, with evident bone growth. Osteogenesis marker (BMP-2) and vascularization marker (VEGF and PDGF) expression in the dual factor group were much better than those of the HA/CS/PCL control group and single factor groups. Collectively, the HA/CS/PCL composite scaffold-engrafting EPCs and BMSCs is effective to repair calvarial defects by regulating endogenous expression of BMP-2, VEGF, and PDGF. Thus, this study provides important implications for the potential clinical application of biomaterial composite scaffold-engrafted engineering cells.

KEYWORDS

HA/CS/PCL composite scaffold, endothelial progenitor cells, bone marrow mesenchymal stem cells, calvarial defect, BMP-2, VEGF, PDGF

Introduction

High incidence diseases such as tumor, trauma, and infection contribute to different degrees of bone defect that cannot be healed by the natural recovery (Baroli, 2009). Biomaterials for bone tissue regeneration and repair are the frontier and hot issue of regenerative medicine research, and scaffold biomaterials are one of the key elements for bone tissue engineering. High biocompatibility, osteogenic ability, and biodegradation are of particular significance for the discovery of scaffold biomaterials. Therefore, there is still a great development for tissue-engineered bone in clinical application (Dumont et al., 2016; Kai et al., 2016).

Hydroxyapatite (HA) is similar to the inorganic components of calvaria in composition and structure, but it is fragile and easy to crack (Oliveira et al., 2017). Chitosan (CS) is a linear natural polysaccharide macromolecule, which has excellent biocompatibility, biodegradability, hydrophilicity, cell affinity, and adhesion (Tian et al., 2022). Polycaprolactone (PCL) is a linear polymer with high mechanical strength and easy processing, and its degradation products are easy to metabolize and eliminate (Lee et al., 2016). HA, CS, and PCL have been applied in bone repair for years. Natural bone tissue is mainly formed by the interaction of nanohydroxyapatite inorganic minerals and collagen organic matter in an orderly arrangement. In order to highly simulate the three-dimensional nanostructure of natural bone, our research group proposed the construction technology of three-component and porous bone composite scaffold containing PCL, CS, and HA and resolved the morphology control of the scaffold by 3D printing (Yu et al., 2020). The biomaterial showed good mechanical properties, bone conductivity, and induction, of which superior mechanical and biological properties displayed a good application prospect for bone defect repair (Gao et al., 2015). However, the biological characteristics of the HA/CS/PCL composite scaffold still need to be evaluated, biocompatibility, effectiveness in loading seed cells, and *in vitro* and *in vivo* osteogenic activity are needed to be tested.

As the seed cells for tissue engineering bone, bone marrow mesenchymal stem cells (BMSCs) are difficult to survive *in vivo*, so that the vascularization could be restricted, which is of decisive significance for bone regeneration and fusion (Stegen et al., 2015). Meanwhile, the endothelial progenitor cells (EPCs) extracted from the peripheral blood and BMSCs are co-cultured together to build a microenvironment in line with the physiological conditions of the human body, which could build the microvasculature by EPCs to supply the blood for the osteogenesis of tissue engineering bone, and promote the survival and osteogenesis of BMSCs (Goerke et al., 2015).

In this study, our research group intended to construct HA/CS/PCL scaffolds inoculating EPCs and BMSCs. In addition, the biocompatibility and bone repair effect of this composite were evaluated, and the effects of this composite on osteogenesis and vascularization using bone morphogenetic protein-2 (BMP-2),

vascular endothelial growth factor (VEGF), and platelet-derived growth factor (PDGF) expression were measured as well.

Materials and methods

Reagents

The chitosan and hydroxyapatite were purchased from Solarbio (Beijing, China), polycaprolactone and simulated body fluid (SBF) from Sigma-Aldrich (Merck KGaA, Darmstadt, Germany), reagents used for cell culture all from Thermo Fisher Scientific (Loughborough, United Kingdom), and CCK-8 reagent from Beyotime (Shanghai, China).

Microscopic examination

The HA/CS/PCL scaffold was observed using the Hitachi S-4300 cold field emission scanning electron microscope (Hitachi, Tokyo, Japan), and its morphology was analyzed with gold coating.

X-ray diffraction study

X-ray diffraction (XRD) of the HA/CS/PCL scaffold was detected using D8 ADVANCE (BRUKER, Germany). JCPDS files 09-0432 were used to confirm the various peaks developed in HA.

Immersion test

The *in vitro* immersion test was conducted to observe and evaluate the degradation behavior of scaffolds in SBF ($M_{\text{SBF}}: M_{\text{scaffold}} = 100:1$), where the scaffolds were dried, weighed, immersed, and incubated with shaking at 100 rpm at 37°C. Every week one scaffold was randomly taken out to weigh the quality to analyze the degradation performance, and the degradation rate was calculated according to the equation, degradation rate = $(M_0 - M)/M_0 \times 100\%$, where M_0 and M are the initial mass and mass at specific time point, respectively.

Cytocompatibility tests

Immersed in DMEM containing 10% FBS ($V_{\text{medium}}: M_{\text{scaffold}} = 10 \text{ ml}:1 \text{ g}$), the scaffold was incubated at 37°C for 120 h in a CO₂ incubator, and then the medium was sterilized with a 0.22- μm micron bacteria-retentive filter to obtain the extracts. Moreover, for the cell viability test, the L929 cells were seeded in 96-well plates, with 2,000 cells/well. After overnight incubation, the medium was replaced with the HA/CS/PCL

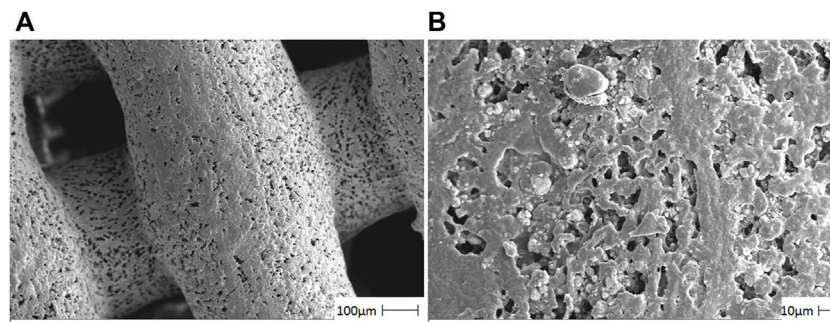


FIGURE 1

Photomicrographs of the HA/CS/PCL composite scaffold material by using a scanning electron microscope. The representative figures were observed on 100 μm (A) and 10 μm (B), respectively.

scaffold extracts (10, 30, 50, and 100%) for 2, 4, and 7 days cell culture. The test of cell viability was performed by CCK-8 kit, according to the manufacturer's instructions.

Animals

Twenty four subjects of this study, New Zealand rabbits, were purchased from Nanchang Longping Rabbit Industry Co., Ltd. with license No. scxk (GAN) 2014-0005. The ethics committee of Hubei University of Medicine approved the animal protocols.

Isolation, culture, and immunophenotyping of BMSCs

After the removal of the femur and tibia, the bone marrow was extruded from the central canal of the bone, and the whole marrow cells were cultured with α -MEM supplemented with 10% fetal bovine serum and antibiotics. By removing the non-adherent cells after 24 h with the medium replacement, BMSCs were obtained and serially subcultured in the ratio of 1:3. BMSCs were used within four passages.

As the adherent cells reach 80%–90% confluence (generally about 10 days), BMSCs were stained with FITC-conjugated CD29 and PE-conjugated CD45 antibodies for 30 min at 4°C and washed with PBS. With at least 10,000 cells per sample analyzed, the expression of cell surface antigens CD29 and CD45 was detected by using a flow cytometer.

Isolation, culture, and immunophenotyping of EPCs

The isolation of EPCs from the bone marrow was made by the lymphocyte separation solution as described previously (Ding

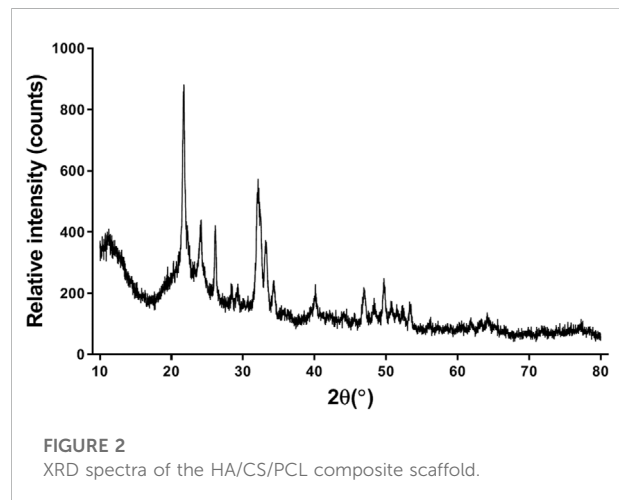


FIGURE 2

XRD spectra of the HA/CS/PCL composite scaffold.

et al., 2019). The isolated cells, incubated in a CO₂ incubator at 37°C, were collected and stained with APC-conjugated CD133 antibody, PE-conjugated CD309 antibody, or PE-conjugated CD34 antibody. After staining for 30 min at 4°C in dark and washing with PBS, the utilization of the flow cytometer helped to detect the CD133, CD309, or CD34 expression of EPCs.

Calvarial defect model

First, rabbits were anesthetized and fixed in the prone position, and they were trephine drilled into the anterior fontanelle with 1-cm diameter. Calvarial defects under copious saline irrigation with care to maintain the dura mater intact. Then, the composite scaffold with presence and absence of engrafted cells was placed in each defect, and the incision was sutured layer-by-layer and wrapped by the sterile dressing. After surgery, all animals were postoperatively cared by monitoring infection and diarrhea with subcutaneous injections of

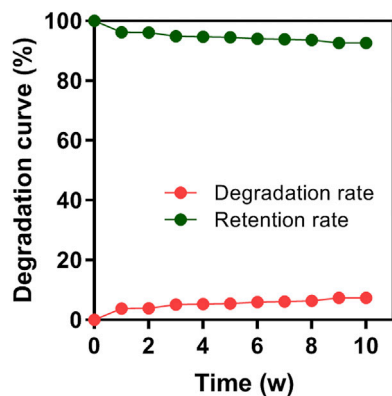


FIGURE 3
Degradation rate of the HA/CS/PCL composite scaffold in 1–10 weeks of immersion in simulated body fluid (SBF).

0.1 mg kg⁻¹ buprenorphine for 3 days and drinking water including trimethoprim–sulfamethoxazole. After 8 weeks, the specimens were harvested for the subsequent examination.

The rabbits were randomly divided into four groups ($n = 6$), namely, as the HA/CS/PCL scaffold group, HA/CS/PCL scaffold + EPCs group, HA/CS/PCL scaffold + BMSCs group, and HA/CS/PCL scaffold + EPCs + BMSCs group. Each piece of scaffold was soaked in cell suspension of the third-generation of BMSCs or EPCs with 0.5×10^6 /ml for 4 h in the CO₂ incubator and before implantation, the scaffolds engrafted cells were washed by PBS. At the post-surgery of the 2nd, 4th, and 8th week, two rabbits ($n = 2$) from each group were randomly chosen for analysis.

X-ray examination

As time progressed to weeks 2, 4, and 6 post-surgery, X-ray examination was performed by an X-ray machine (OEC9800,

Shanghai Xianwei Optoelectronic Technology Co., Ltd.) to observe the repair of calvarial defects.

Micro-CT

At the post-surgery of the 2nd, 4th, and 8th week, approximating images of calvaria with new bone deposition were reconstructed by three-dimensional micro-computerized tomography (micro-CT), whose scanning parameters are 80kV, 500 μ A, and resolution of 27 μ M, and the reestablishment of three-dimensional (3D) images and volumetric analysis were performed by the Inveon Research Workplace 2.2. Bone volume (BV) and tissue volume (TV) were used to quantify the calvaria with new bone, and their percentages of bone volume (BV/TV) of each graft site were measured.

Hematoxylin and eosin (H&E) staining

After micro-CT imaging, the calvaria were decalcified for 5 weeks. The specimens of the calvarial defect region were dehydrated and embedded in paraffin and sectioned coronally with 5- μ m thickness. The sections were stained with hematoxylin and eosin to visualize tissue structure.

Western blot

The extraction of total protein from the bone tissues in the defect areas of the calvaria was performed by using the triplePrep kit (GE Healthcare Life Sciences), and its concentration was determined with a BCA assay kit. 25 μ g protein per sample was separated *via* 10% SDS-PAGE and transferred to the PVDF membrane as described (Luo et al., 2021). After blocking in 5% skim milk at room temperature for 2 h, PVDF membranes were treated with the following primary antibodies overnight at

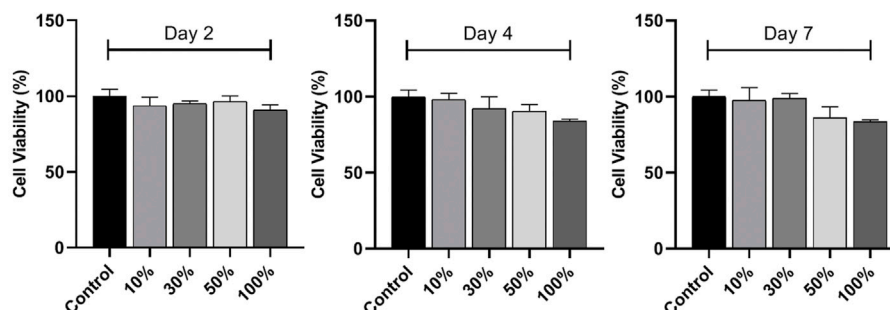
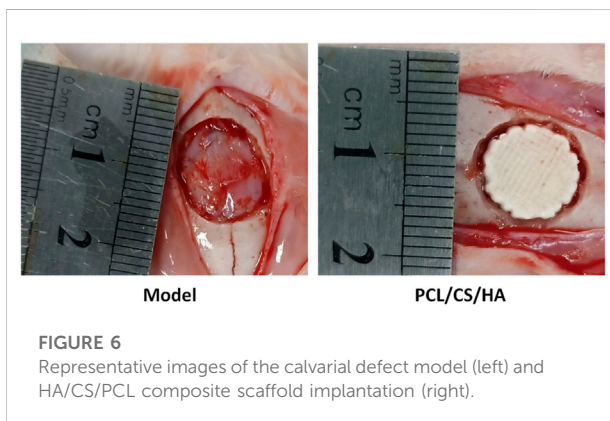
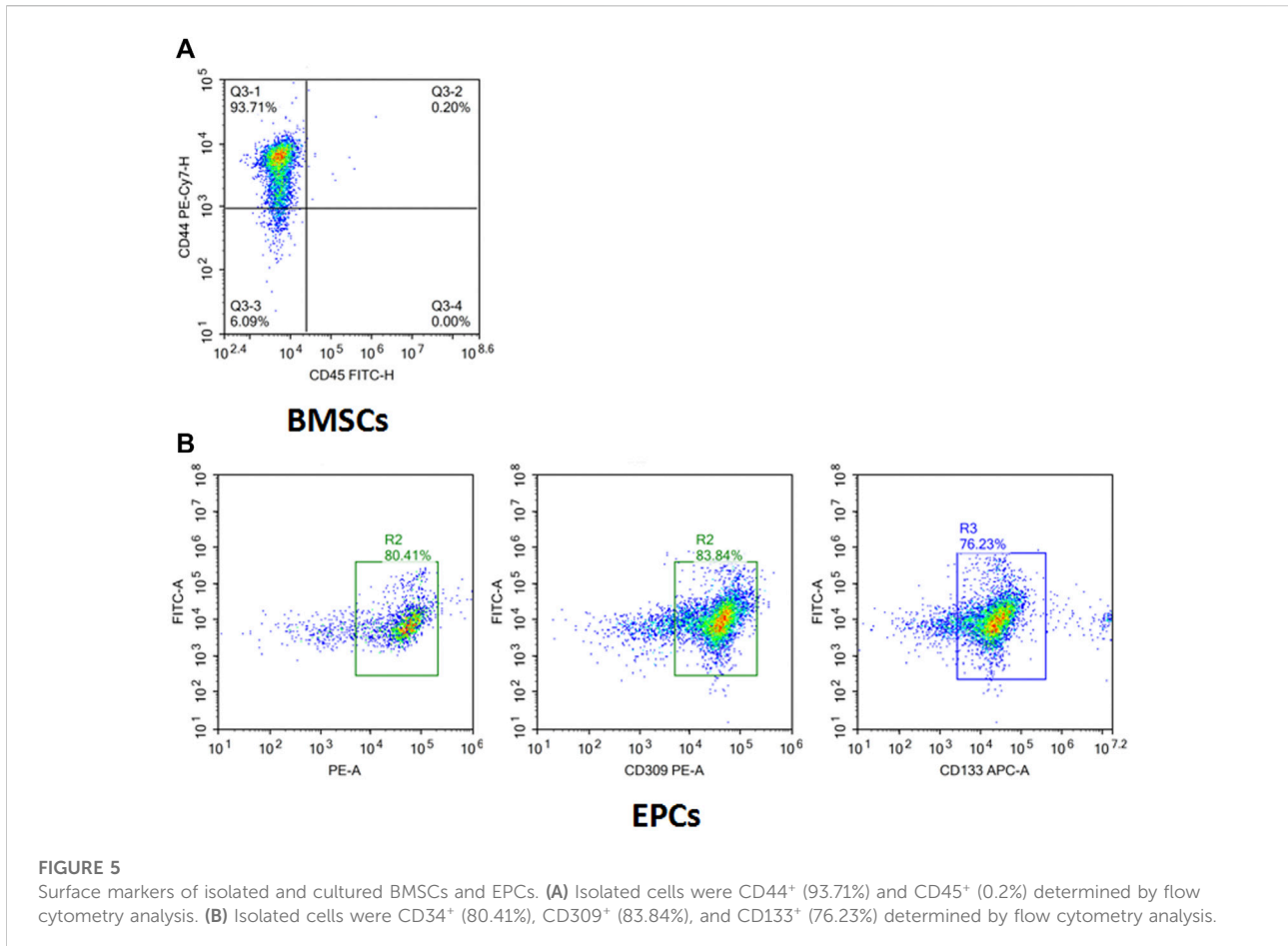


FIGURE 4
In vitro cytocompatibility of the HA/CS/PCL scaffold. CCK-8 assay of L929 cell proliferation on the HA/CS/PCL scaffold after 2, 4, and 7 days incubation. The data represent the mean \pm SD.



Touch Imaging System—Bio-Rad Laboratories (Bio-Rad Lab, Hercules, CA, United States).

Statistical analysis

All the data were presented as mean and standard deviation and analyzed by SPSS 19.0. Overall significant differences among groups were determined by one-way ANOVA. When overall analysis demonstrated the presence of significant differences among all of the different groups studied, the differences between specific groups were tested using a *post-hoc* analysis, Tukey's test. $p < 0.05$ was set as the threshold to indicate significant difference between groups.

Results

SEM ultrastructure analysis

In [Figure 1](#), the HA/CS/PCL scaffold showed the neatly arranged fibers composed of CS and PCL in grid shape with

4°C, rabbit polyclonal anti-BMP-2 (1:1000, bs-1012R, Bioss), rabbit polyclonal anti-VEGF (1:1000, bs-1313R, Bioss), and rabbit polyclonal anti-PDGFR (1:1000, bs-0196R, Bioss), followed by incubation with HRP-labeled IgG at 37°C for 2 h. The western blots were stained with an ECL reagent (Santa Cruz Biotech, CA, United States) and visualized by the ChemiDoc

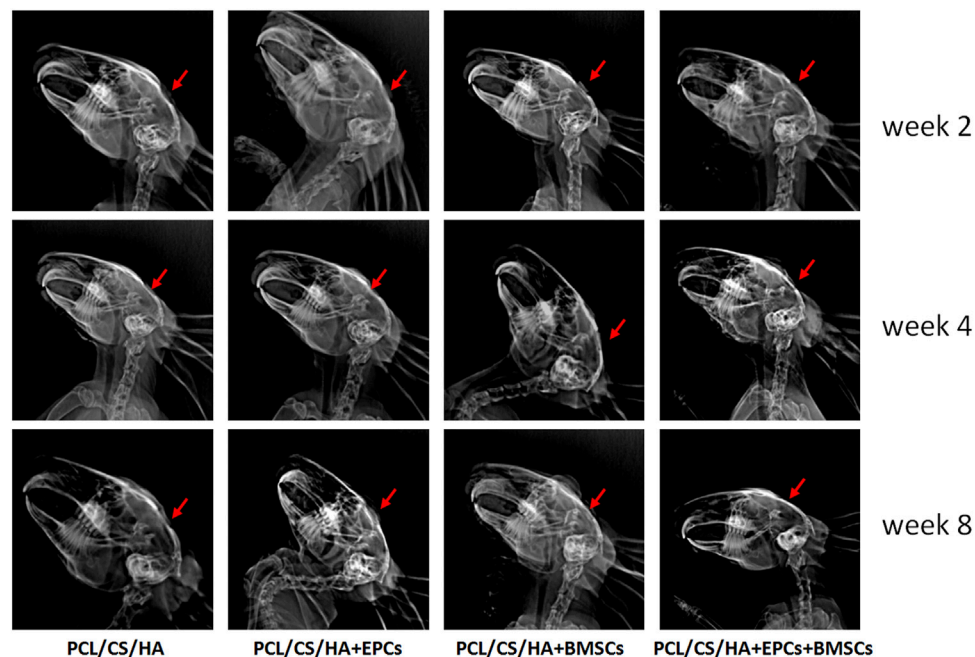


FIGURE 7

Evaluation of calvarial repair by X-ray images after 2, 4, and 8 weeks of implantation. The red arrow indicates the defect area receiving scaffold implantation.

an average pore size of about 250 μm . HA distributed evenly on the fiber surface in granular form, which proved that the ternary composite presented uniform and loose macroporous structure.

XRD analysis

For the HA/CS/PCL composite scaffold, peaks corresponding to HA crystalline phases appeared (Figure 2). The peaks of HA match well with JCPDS No. 09-0432. It indicated that the scaffold was combined with HA, CS, and PCL by physical interaction, which did not affect the biological function of HA.

In vitro degradation behavior

After 10 consecutive weeks, the degradation rate of the HA/CS/PCL composite scaffold in SBF was 7.39%, indicating that the HA/CS/PCL scaffold possessed certain mechanical stability and degraded slowly over time (Figure 3). This property meets the degradation and mechanical performance requirements of the biomaterial scaffold.

In vitro cytocompatibility of HA/CS/PCL scaffold

L929 is the earliest and most widely used cell line in the cytotoxicity test because of its stable passage, rapid propagation, and low culture conditions *in vitro*. The cell viabilities were above 80% after 2, 4, and 7 days cell culture in the scaffold extracts compared with that of the blank control, indicating non-cytotoxicity and acceptable cytocompatibility of the scaffolds, according to the criteria for the evaluation of cell toxicity test recommended in GB/T16886.5-1997-ISO10993-5:1992 (Figure 4).

Identification of BMSCs and EPCs

The flow cytometry results (Figure 5A) showed the cell surface antigen profile of BMSCs, which was identified that 93.71% of the cells expressed CD44, but was homogeneously negative for CD45 (0.2%). It confirmed the identification of isolated BMSCs. In addition to BMSCs, the isolated cells were positive for EPCs markers CD34 (80.41%), CD133 (83.84%), and CD309 (76.23%) (Figure 5B), which manifested that EPCs were successfully separated from rabbit bone marrow by the Ficoll density gradient method.

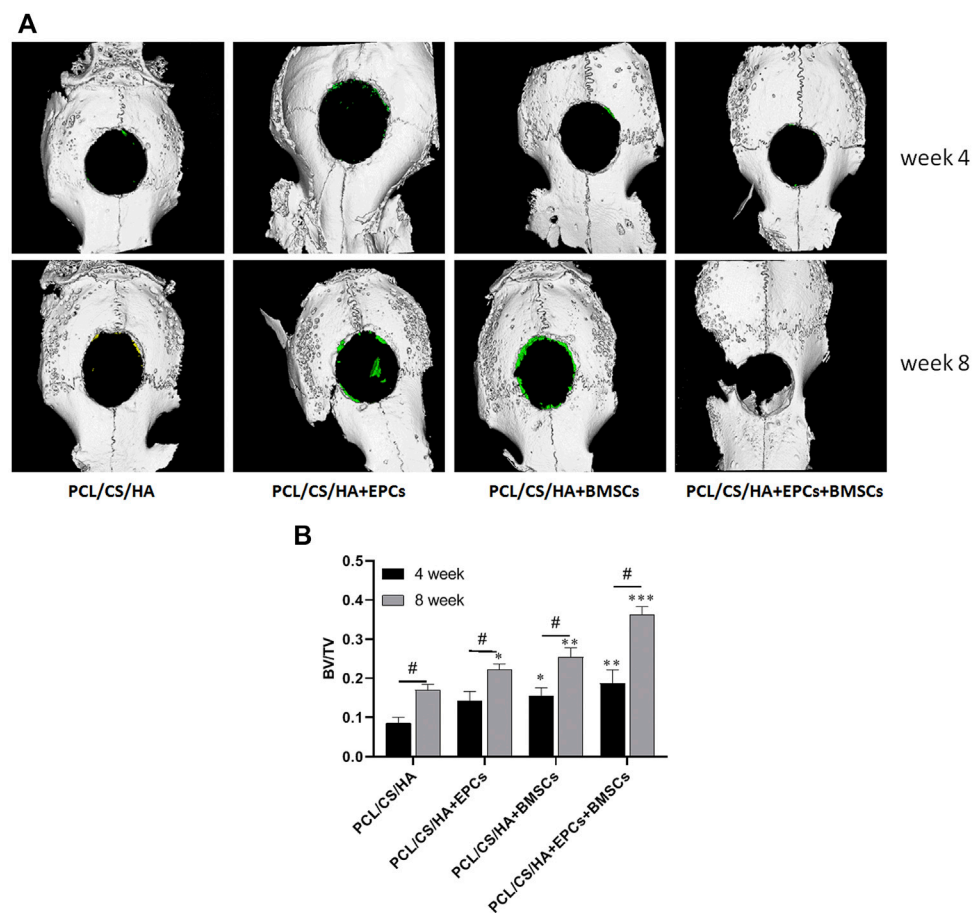


FIGURE 8

Three-dimensional micro-CT images of calvarial defect areas. The representative images (A) of micro-CT reconstruction and the quantitative data of BV/TV (B) from micro-CT evaluations of the four groups. * $p < 0.05$, ** $p < 0.01$, *** $p < 0.001$ vs. HA/CS/PCL group (the same time point), # $p < 0.05$.

Calvarial defect model and scaffold implantation

As shown in Figure 6, after the composite scaffold was implanted into the calvaria, none of the rabbits died throughout the experiment, and all rabbits were under healthy conditions without infection or ulceration in the wound.

EPCs and BMSCs improved the *in vivo* performance of HA/CS/PCL

As shown in Figure 7, HA/CS/PCL + EPCs, HA/CS/PCL + BMSCs, and HA/CS/PCL + EPCs + BMSCs, presenting obvious repair on the injured calvaria of rabbits, were more remarkable compared with HA/CS/PCL at the 8th week after scaffold implantation.

EPCs and BMSCs accelerates HA/CS/PCL-based new bone formation

As shown in Figure 8A, compared with the HA/CS/PCL, BV/TV of HA/CS/PCL + EPCs, HA/CS/PCL + BMSCs, and HA/CS/PCL + EPCs + BMSCs groups increased significantly after 4 weeks and 8 weeks ($p < 0.05$), and the HA/CS/PCL + EPCs + BMSCs group presented the best calvarial repair effect at both the 4th and 8th week (Figure 8B).

EPCs and BMSCs improves the histological repair results of calvarial defects

As shown in Figure 9, by the 2nd week, all the groups failed to form bone after implantation. By the 4th week, connective tissue (CT) was found around the HA/CS/PCL composite scaffold,

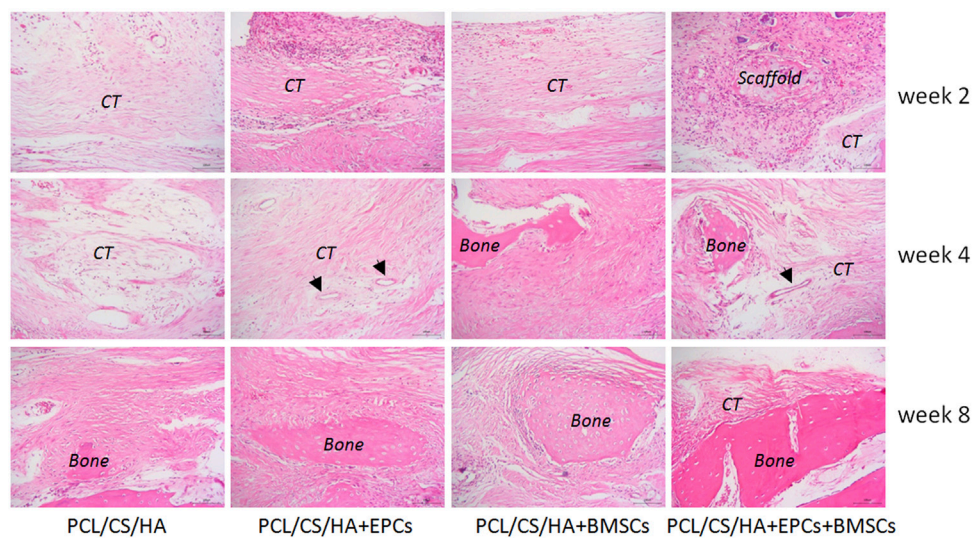


FIGURE 9

Histological structure of defected calvaria with composite scaffold repair at the post-surgery of the 2nd, 4th, and 8th week. New bone (bone), connective tissue (CT), and arrows indicate blood vessel.

while there was significantly more CT in the HA/CS/PCL + EPCs + BMSCs group than those of the other three groups. New blood vessels could be found even in the HA/CS/PCL + EPCs and HA/CS/PCL + EPCs + BMSCs groups. By 8 weeks, new bone was observed in all the groups. Moreover, implantation of the composite scaffold of HA/CS/PCL, at calvarial defect site, performed moderate bone regeneration, but failed to completely repair the defects, while implantation of HA/CS/PCL + BMSCs and HA/CS/PCL + EPCs composite scaffolds, there were more new bone in the calvarial defect area, however, the HA/CS/PCL + EPCs + BMSCs composite scaffold resulted in the most significant repair of the defects.

EPCs and BMSCs enhances the expression of BMP-2, VEGF, and PDGF

As shown in Figure 10, compared with the HA/CS/PCL group, BMP-2 expression in the HA/CS/PCL + BMSCs and HA/CS/PCL + EPCs + BMSCs groups was significantly higher at the 2nd and 4th week ($p < 0.05$). The HA/CS/PCL + EPCs, HA/CS/PCL + BMSCs, and HA/CS/PCL + EPCs + BMSCs groups all showed remarkably higher levels of BMP-2 at the 8th week compared with the HA/CS/PCL group ($p < 0.05$).

VEGF levels in the HA/CS/PCL + BMSCs and HA/CS/PCL + EPCs + BMSCs groups were greatly higher than that in the HA/CS/PCL group at the 2nd week ($p < 0.05$). At the 4th week, VEGF expression in the HA/CS/PCL + EPCs + BMSCs group exceeded that in the HA/CS/PCL group ($p < 0.05$). At the 8th week, VEGF

expression in the HA/CS/PCL + BMSCs and HA/CS/PCL + EPCs + BMSCs groups were significantly higher than that in the HA/CS/PCL group ($p < 0.05$), which indicated potential neovascularization ability of HA/CS/PCL scaffolds engrafted BMSCs or EPCs.

The expression of PDGF in the HA/CS/PCL + EPCs, HA/CS/PCL + BMSCs, and HA/CS/PCL + EPCs + BMSCs groups increased remarkably at the 2nd, 4th, and 8th week compared with the HA/CS/PCL group ($p < 0.05$).

Discussion

In this study, the composite scaffolds engrafted EPCs and BMSCs were developed, of which function in the calvarial repair was confirmed. Moreover, this study, providing the new experimental evidence for the treatment of calvarial repair, presented that the HA/CS/PCL scaffold possessed a mild repair effect, while the inoculation with EPCs and BMSCs obviously promoted the calvarial repair.

It has been found in our previous study that BMSCs possess the ability of directional migration by microphotography, which lays the foundation for the construction of tissue-engineered bone in this present study (Yang et al., 2014). Niemyer et al. (2010) reported that human mesenchymal stem cells were transplanted into the critical-size bone defect of rabbit to examine the regeneration potential. Zong et al. (2010) evaluated the osteogenic effect of BMSCs and osteoblast-like cells combined with poly lactic-co-glycolic acid (PLGA) on

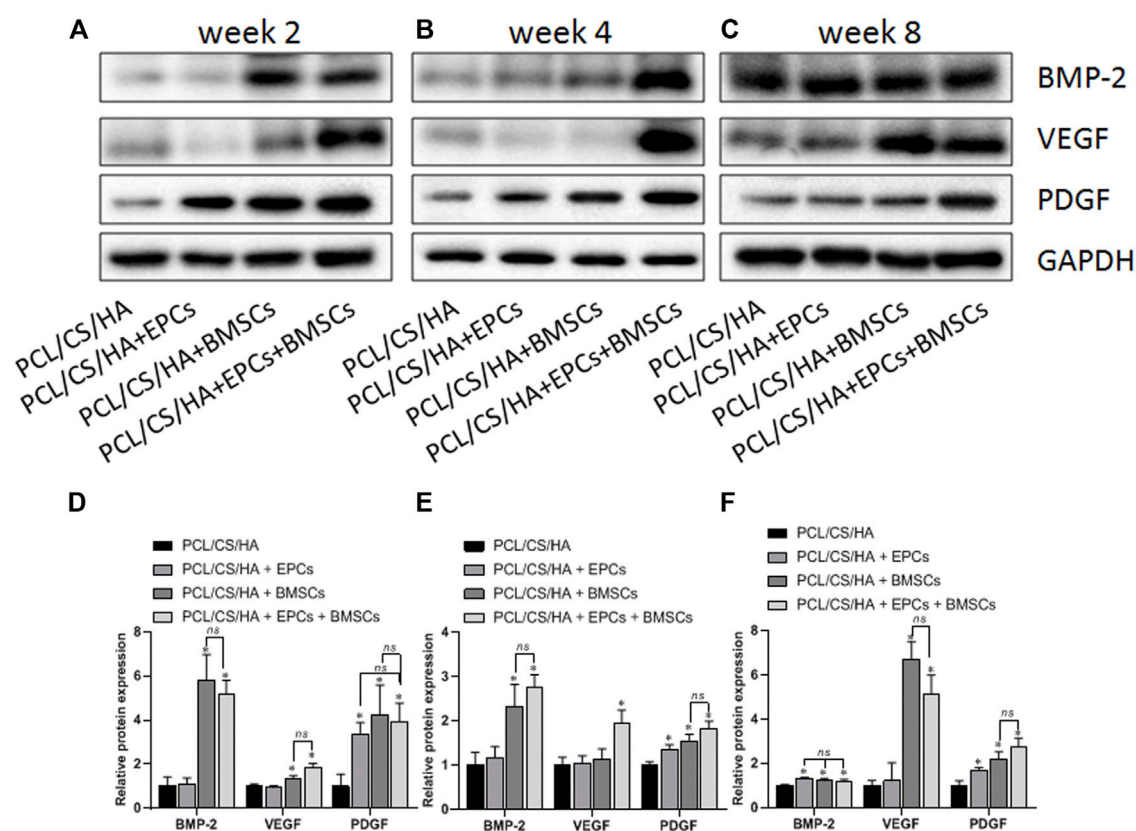


FIGURE 10

Expression levels of BMP-2, VEGF, and PDGF in the repaired calvaria with composite scaffold by western blot analysis. The representative bands and the quantified gray scale normalized to GAPDH for BMP-2, VEGF, and PDGF expression at the 2nd week (A,D), 4th week (B,E), and 8th week (C,F). * $p < 0.05$ vs. HA/CS/PCL group, ns $p > 0.05$.

the calvarial defect of rats and revealed that BMSCs were superior to osteoblasts in bone reconstruction. In this study, BMSCs and EPCs were isolated and identified on the basis of the surface markers and were used as seed cells, and then the reconstruction effects were evaluated on the calvarial defect of rabbits by BMSCs, EPCs, or combined BMSCs and EPCs in HA/CS/PCL scaffolds.

Scaffold material plays a crucial role in bone tissue engineering not only in supporting and maintaining the shape of original bone tissue but also as a biomaterial template providing attachment for engrafted cells to live, grow, and differentiate, and guiding the regeneration of damaged tissue and controlling the regenerated structure (Szpalski et al., 2012). In this study, the HA/CS/PCL porous ternary composite scaffold was prepared by three-dimensional printing and molding technology. As the scaffold was effectively solved by the three-dimensional and controllable internal and external structures, the obtained multi-scale structure and shape of scaffolds could be used to simulate the ideal bone repair material. Some studies have

shown that scaffold using calcium-deficient hydroxyapatite and BMP-2-loaded sulfate chitosan could repair rat calvarial defect and promote new bone formation *in vivo* (Zhao et al., 2012). Chen et al. (2013) used macroporous calcium phosphate seeded with human umbilical cord mesenchymal stem cells to repair 8-mm rat cranial defects, which promoted new bone regeneration. In this study, X-ray, micro-CT, and pathological results manifested that HA/CS/PCL + EPCs, HA/CS/PCL + BMSCs, and HA/CS/PCL + EPCs + BMSCs groups had remarkable repair effect on bone defects. Particularly, at the 8th week, HA/CS/PCL + EPCs + BMSCs scaffold implantation performed more significantly. These results suggest that BMSCs may be combined with EPCs as seed cells, which possess neovascularization ability, to exert both the directional migration ability of BMSCs and the vascularization ability of EPCs to facilitate new bone formation.

The differentiation of BMSCs into osteoblast-like cells, osteogenesis induction by BMP-2 is of importance for improving the osteoinduction and osteoconduction properties

of bone scaffold materials (Yamaguchi et al., 1996; Partridge et al., 2002; Li et al., 2006). The new bone formation by scaffold materials promotes vascularization, depending on the participation of growth factors, such as VEGF, PDGF (Nguyen et al., 2012), and transforming growth factor β (TGF- β) (Thurston, 2002). BMP is the main signaling pathway in osteogenic differentiation to boost the formation of new bone (Liu et al., 2017). As the strongest member in bone induction in the BMP family (Sun et al., 2017), BMP-2 can promote bone formation by direct application or local application in carriers (Demiray et al., 2017; Khorsand et al., 2017; Kuttappan et al., 2018) and enhance the expression of Runx2, a key transcription factor in bone differentiation, thus to activate the osteogenic process (Li et al., 2017). VEGF is recognized as the most powerful and specific angiogenic factor (Ju et al., 2018), which regulates bone formation by stimulating the differentiation and proliferation of osteoblasts, accelerating the formation and remodeling of bone (Huang et al., 2016). Both BMP-2 and VEGF play the important roles in bone regeneration as osteogenic factors and angiogenic factors, respectively (Kempen et al., 2009). It is reported that the expression of BMP-2 and VEGF enhance each other in the fracture healing (Zhang et al., 2011). VEGF could upregulate the expression of BMP-2 in osteoblasts and accelerate bone healing (Samee et al., 2008). In the initial steps of bone regeneration, PDGF promotes mitosis and angiogenesis, increases the synthesis of collagen and strengthens the local stress (Yang et al., 2017). Nash et al. (1994) injected collagen-containing rhPDGF into rabbits that underwent unilateral tibial osteotomy and found that rhPDGF increased the callus density, callus volume, and osteogenic differentiation. This present study showed that the expression of BMP-2, VEGF, and PDGF in the HA/CS/PCL + EPCs + BMSCs group increased at the 2nd, 4th, and 8th weeks, and there was a clear improvement in new bone formation and pathological change compared with the other three groups, which suggest that the better effect of HA/CS/PCL + EPCs + BMSCs on repairing bone defects may be related to the significantly increased expression of BMP-2, VEGF, and PDGF and their additive effect on bone regeneration.

In conclusion, this study proves that HA/CS/PCL + EPCs + BMSCs possess a better bone repair effect in the rabbit calvarial injury model, likely through increasing the expression of BMP-2, VEGF, and PDGF and, simultaneously, provides the experimental evidence for the future clinical application of the cell-matrix composite scaffold.

References

- Baroli, B. (2009). From natural bone grafts to tissue engineering therapeutics: Brainstorming on pharmaceutical formulative requirements and challenges. *J. Pharm. Sci.* 98 (4), 1317–1375. doi:10.1002/jps.21528
- Chen, W., Liu, J., Manuchehrabadi, N., Weir, M. D., Zhu, Z., Xu, H. H., et al. (2013). Umbilical cord and bone marrow mesenchymal stem cell

Data availability statement

The original contributions presented in the study are included in the article/Supplementary Material; further inquiries can be directed to the corresponding authors.

Ethics statement

The animal study was reviewed and approved by the ethics committee of Hubei University of Medicine.

Author contributions

HY and WL conceived and designed the experiments. HY, LX, XL, YC, LZ, XN, and JL performed the experiments and analyzed the data. HY, JL, and WL wrote the manuscript. All authors read and approved the manuscript and agree to be accountable for all aspects of the research in ensuring that the accuracy or integrity of any part of the work are appropriately investigated and resolved.

Funding

This study was supported by the National Natural Science Foundation of China (No. 81671831).

Conflict of interest

The authors declare that the research was conducted in the absence of any commercial or financial relationships that could be construed as a potential conflict of interest.

Publisher's note

All claims expressed in this article are solely those of the authors and do not necessarily represent those of their affiliated organizations, or those of the publisher, the editors, and the reviewers. Any product that may be evaluated in this article, or claim that may be made by its manufacturer, is not guaranteed or endorsed by the publisher.

seeding on macroporous calcium phosphate for bone regeneration in rat cranial defects. *Biomaterials* 34 (38), 9917–9925. doi:10.1016/j.biomaterials.2013.09.002

Demiray, S. B., Yilmaz, O., Goker, E., Tavmergen, E., Calimlioglu, N., Sezerman, U., et al. (2017). Expression of the bone morphogenetic protein-2 (BMP2) in the

- human cumulus cells as a biomarker of oocytes and embryo quality. *J. Hum. Reprod. Sci.* 10 (3), 194. doi:10.4103/jhrs.JHRS_21_17
- Ding, P., Zhang, W., Tan, Q., Yao, C., and Lin, S. (2019). Impairment of circulating endothelial progenitor cells (EPCs) in patients with glucocorticoid-induced avascular necrosis of the femoral head and changes of EPCs after glucocorticoid treatment *in vitro*. *J. Orthop. Surg. Res.* 14 (1), 226. doi:10.1186/s13018-019-1279-6
- Dumont, V. C., Mansur, H. S., Mansur, A. A., Carvalho, S. M., Capanema, N. S., Barrioni, B. R., et al. (2016). Glycol chitosan/nanohydroxyapatite biocomposites for potential bone tissue engineering and regenerative medicine. *Int. J. Biol. Macromol.* 93 (Pt B), 1465–1478. doi:10.1016/j.ijbiomac.2016.04.030
- Gao, G., Lu, S., Dong, B., Zhang, Z., Zheng, Y., Ding, S., et al. (2015). One-pot synthesis of carbon coated Fe₃O₄ nanosheets with superior lithium storage capability. *J. Mat. Chem. A Mat.* 3 (8), 4716–4721. doi:10.1039/C4TA05725B
- Goerke, S. M., Obermeyer, J., Plaha, J., Stark, G. B., and Finkenzeller, G. (2015). Endothelial progenitor cells from peripheral blood support bone regeneration by provoking an angiogenic response. *Microvasc. Res.* 98, 40–47. doi:10.1016/j.mvr.2014.12.001
- Huang, Y., Wu, G., Dou, Y., and Cao, S. (2016). Mechanism of Shensu IV intervention on podocyte injury in rats with puromycin nephropathy. *Shanxi Zhongyi* 37, 1559–1562. doi:10.1042/BSR20203362
- Ju, X., Xue, D., Wang, T., Ge, B., Zhang, Y., Li, Z., et al. (2018). Catalpol promotes the survival and VEGF secretion of bone marrow-derived stem cells and their role in myocardial repair after myocardial infarction in rats. *Cardiovasc. Toxicol.* 18 (5), 471–481. doi:10.1007/s12012-018-9460-4
- Kai, D., Prabhakaran, M. P., Chan, B. Q., Liow, S. S., Ramakrishna, S., Xu, F., et al. (2016). Elastic poly(ϵ -caprolactone)-polydimethylsiloxane copolymer fibers with shape memory effect for bone tissue engineering. *Biomed. Mat.* 11 (1), 015007. doi:10.1088/1748-6041/11/1/015007
- Kempen, D. H., Lu, L., Heijink, A., Hefferan, T. E., Creemers, L. B., Maran, A., et al. (2009). Effect of local sequential VEGF and BMP-2 delivery on ectopic and orthotopic bone regeneration. *Biomaterials* 30 (14), 2816–2825. doi:10.1016/j.biomaterials.2009.01.031
- Khorsand, B., Elangovan, S., Hong, L., Dewerth, A., Kormann, M. S., Salem, A. K., et al. (2017). A comparative study of the bone regenerative effect of chemically modified RNA encoding BMP-2 or BMP-9. *AAPS J.* 19 (2), 438–446. doi:10.1208/s12248-016-0034-8
- Kuttappan, S., Anitha, A., Minsha, M. G., Menon, P. M., Sivanarayanan, T. B., Vijayachandran, L. S., et al. (2018). BMP2 expressing genetically engineered mesenchymal stem cells on composite fibrous scaffolds for enhanced bone regeneration in segmental defects. *Mater. Sci. Eng. C* 85, 239–248. doi:10.1016/j.msec.2018.01.001
- Lee, S. J., Lee, D., Yoon, T. R., Kim, H. K., Jo, H. H., Park, J. S., et al. (2016). Surface modification of 3D-printed porous scaffolds via mussel-inspired polydopamine and effective immobilization of rhBMP-2 to promote osteogenic differentiation for bone tissue engineering. *Acta biomater.* 40, 182–191. doi:10.1016/j.actbio.2016.02.006
- Li, C., Vepari, C., Jin, H. J., Kim, H. J., and Kaplan, D. L. (2006). Electrospun silk-BMP-2 scaffolds for bone tissue engineering. *Biomaterials* 27 (16), 3115–3124. doi:10.1016/j.biomaterials.2006.01.022
- Li, Z., Wang, W., Xu, H., Ning, Y., Fang, W., Liao, W., et al. (2017). Effects of altered CXCL12/CXCR4 axis on BMP2/Smad/Runx2/Osterix axis and osteogenic gene expressions during osteogenic differentiation of MSCs. *Am. J. Transl. Res.* 9 (4), 1680–1693.
- Liu, J., Liang, C., Guo, B., Wu, X., Li, D., Zhang, Z., et al. (2017). Increased PLEKHO1 within osteoblasts suppresses Smad-dependent BMP signaling to inhibit bone formation during aging. *Aging Cell.* 16 (2), 360–376. doi:10.1111/acel.12566
- Luo, T., Fu, X., Liu, Y., Ji, Y., and Shang, Z. (2021). Sulforaphane inhibits osteoclastogenesis via suppression of the autophagic pathway. *Mol. (Basel, Switz.)* 26 (2), 347. doi:10.3390/molecules26020347
- Nash, T. J., Howlett, C. R., Martin, C., Steele, J., Johnson, K. A., Hicklin, D. J., et al. (1994). Effect of platelet-derived growth factor on tibial osteotomies in rabbits. *Bone* 15 (2), 203–208. doi:10.1016/8756-3282(94)90709-9
- Nguyen, L. H., Annabi, N., Nikkhal, M., Bae, H., Binan, L., Park, S., et al. (2012). Vascularized bone tissue engineering: Approaches for potential improvement. *Tissue Eng. Part B Rev.* 18 (5), 363–382. doi:10.1089/ten.TEB.2012.0012
- Niemeyer, P., Szalay, K., Luginbühl, R., Südkamp, N. P., and Kasten, P. (2010). Transplantation of human mesenchymal stem cells in a non-autogenous setting for bone regeneration in a rabbit critical-size defect model. *Acta biomater.* 6 (3), 900–908. doi:10.1016/j.actbio.2009.09.007
- Oliveira, H. L., Da Rosa, W., Cuevas-Suárez, C. E., Carreño, N., da Silva, A. F., Guim, T. N., et al. (2017). Histological evaluation of bone repair with hydroxyapatite: A systematic review. *Calcif. Tissue Int.* 101 (4), 341–354. doi:10.1007/s00223-017-0294-z
- Partridge, K., Yang, X., Clarke, N. M., Okubo, Y., Bessho, K., Sebald, W., et al. (2002). Adenoviral BMP-2 gene transfer in mesenchymal stem cells: *In vitro* and *in vivo* bone formation on biodegradable polymer scaffolds. *Biochem. Biophysical Res. Commun.* 292 (1), 144–152. doi:10.1006/bbr.2002.6623
- Samee, M., Kasugai, S., Kondo, H., Ohya, K., Shimokawa, H., Kuroda, S., et al. (2008). Bone morphogenetic protein-2 (BMP-2) and vascular endothelial growth factor (VEGF) transfection to human periosteal cells enhances osteoblast differentiation and bone formation. *J. Pharmacol. Sci.* 108 (1), 18–31. doi:10.1254/jphs.08036fp
- Stegen, S., van Gestel, N., and Carmeliet, G. (2015). Bringing new life to damaged bone: The importance of angiogenesis in bone repair and regeneration. *Bone* 70, 19–27. doi:10.1016/j.bone.2014.09.017
- Sun, J., Zhang, Y., Li, B., Gu, Y., and Chen, L. (2017). Controlled release of BMP-2 from a collagen-mimetic peptide-modified silk fibroin-nanohydroxyapatite scaffold for bone regeneration. *J. Mat. Chem. B* 5 (44), 8770–8779. doi:10.1039/c7tb02043k
- Szpalski, C., Wetterau, M., Barr, J., and Warren, S. M. (2012). Bone tissue engineering: Current strategies and techniques—Part I: Scaffolds. *Tissue Eng. Part B Rev.* 18 (4), 246–257. doi:10.1089/ten.TEB.2011.0427
- Thurston, G. (2002). Complementary actions of VEGF and angiopoietin-1 on blood vessel growth and leakage. *J. Anat.* 200 (6), 575–580. doi:10.1046/j.1469-7580.2002.00061.x
- Tian, Y., Wu, D., Wu, D., Cui, Y., Ren, G., Wang, Y., et al. (2022). Chitosan-based biomaterial scaffolds for the repair of infected bone defects. *Front. Bioeng. Biotechnol.* 10, 899760. doi:10.3389/fbioe.2022.899760
- Yamaguchi, A., Ishizuya, T., Kintou, N., Wada, Y., Katagiri, T., Wozney, J. M., et al. (1996). Effects of BMP-2, BMP-4, and BMP-6 on osteoblastic differentiation of bone marrow-derived stromal cell lines, ST2 and MC3T3-G2/PA6. *Biochem. Biophysical Res. Commun.* 220 (2), 366–371. doi:10.1006/bbr.1996.0411
- Yang, X., Dong, M., Wen, H., Liu, X., Zhang, M., Ma, L., et al. (2017). MiR-26a contributes to the PDGF-BB-induced phenotypic switch of vascular smooth muscle cells by suppressing Smad1. *Oncotarget* 8 (44), 75844–75853. doi:10.18632/oncotarget.17998
- Yang, Z. S., Tang, X. J., Guo, X. R., Zou, D. D., Sun, X. Y., Feng, J. B., et al. (2014). Cancer cell-oriented migration of mesenchymal stem cells engineered with an anticancer gene (PTEN): An imaging demonstration. *Oncotargets. Ther.* 7, 441–446. doi:10.2147/OTT.S59227
- Yu, H. D., Zhang, L., Xia, L. Y., Mao, M., Ni, X. B., Leng, W. D., et al. (2020). Construction and characterization of nano-hydroxyapatite/chitosan/polycaprolactone composite scaffolds by 3D printing. *Chin. J. Tissue Eng. Res.* 24 (10), 1496–1501. doi:10.3969/j.issn.2095-4344.2238
- Zhang, W., Wang, X., Wang, S., Zhao, J., Xu, L., Zhu, C., et al. (2011). The use of injectable sonication-induced silk hydrogel for VEGF(165) and BMP-2 delivery for elevation of the maxillary sinus floor. *Biomaterials* 32 (35), 9415–9424. doi:10.1016/j.biomaterials.2011.08.047
- Zhao, J., Shen, G., Liu, C., Wang, S., Zhang, W., Zhang, X., et al. (2012). Enhanced healing of rat calvarial defects with sulfated chitosan-coated calcium-deficient hydroxyapatite/bone morphogenetic protein 2 scaffolds. *Tissue Eng. Part A* 18 (1–2), 185–197. doi:10.1089/ten.TEA.2011.0297
- Zong, C., Xue, D., Yuan, W., Wang, W., Shen, D., Tong, X., et al. (2010). Reconstruction of rat calvarial defects with human mesenchymal stem cells and osteoblast-like cells in poly-lactic-co-glycolic acid scaffolds. *Eur. Cell. Mat.* 20, 109–120. doi:10.22203/ecm.v020a10